



ELSEVIER

Journal of Alloys and Compounds 330–332 (2002) 727–731

Journal of
ALLOYS
AND COMPOUNDS

www.elsevier.com/locate/jallcom

Structure of nanocomposite metal hydrides[☆]

J. Huot^{a,*}, J.F. Pelletier^b, G. Liang^a, M. Sutton^b, R. Schulz^{a,b}^aHydro-Québec Research Institute, 1800 Blvd. Lionel-Boulet, Varennes, Québec, Canada J3X 1S1^bCentre for the Physics of Materials, McGill University, Montreal, Québec, Canada H3A 2T8

Abstract

It has recently been shown that MgH₂–(V, Nb) nanocomposite has very fast hydrogen sorption kinetics. This could be explained by the presence of vanadium which eases hydrogen penetration into the material and by the particular microstructure of this nanocomposite. In order to have a better understanding of the nature and hydrogen desorption mechanism, a systematic structural study has been undertaken. The powder morphology and chemical phase distribution were observed by SEM. X-ray diffraction under hydrogen pressure was performed at different temperatures in order to see the effect of absorption/desorption process on the crystal structure. Crystallite size was evaluated by X-ray powder diffraction peak broadening. Real time X-ray investigations of hydrogen desorption in MgH₂–Nb nanocomposite were performed using synchrotron radiation. For the first time, we were able to get direct evidence of the dehydrogenation mechanism. A metastable new niobium hydride phase associated with the desorption process was detected. This metastable hydride is probably the result of long-range ordering of hydrogen in the niobium hydride lattice in order to facilitate the hydrogen flow. © 2002 Elsevier Science B.V. All rights reserved.

Keywords: Nanocomposite; Magnesium hydride; Dehydrogenation mechanism; Synchrotron

1. Introduction

Magnesium is an attractive material for hydrogen storage applications because of its low cost and high hydrogen capacity. Unfortunately, because of its high temperature of operation (plateau pressure of 1 bar at 552 K) and slow sorption kinetics, practical applications using magnesium-based alloys have been limited. Also, preparation of Mg-based alloys by conventional metallurgical procedures is difficult because of the low melting point and high vapor pressure of magnesium [1]. However, it has recently been found that improved hydrogen sorption kinetics could be achieved by ball milling pure magnesium [2] or magnesium hydride [3–5]. Much better kinetics were obtained by ball milling magnesium hydride and 3d-transition elements to form nanocomposites [6]. These nanocomposites showed essentially the same formation enthalpy and entropy as pure magnesium hydride. However, the activation energy of desorption was drastically reduced [6]. Nanocomposites with V as additive showed very fast desorption kinetics above 523 K and were able to absorb hydrogen at a temperature as low as 302 K.

The hydrogen storage properties of MgH₂–V nanocomposite were reported in a series of articles [7–9]. First, it was shown that the overall reaction during milling is:



The fast kinetics were explained by a variety of factors such as: reduction of activation energy, introduction of defects by intensive milling, increase of specific surface area, small effective particle size and particular microstructure of the composite [7]. Hydrogen desorption at high temperature and high driving force is controlled by the interface (Mg/MgH₂) motion, while for small driving force, the nucleation and growth control the early stage of desorption and long range hydrogen diffusion controls the later stage. Below 523 K, nucleation and growth dominate the hydrogen desorption [8]. Influence of cycling was studied and no significant change in hydriding/dehydriding kinetics at 573 K was found. A good resistance to decrepitation was also observed [9].

Although hydrogen sorption properties of MgH₂–V nanocomposite have been well characterized, the exact desorption mechanism is still not well defined. Because niobium is a better X-ray scatterer than vanadium, and MgH₂+5at.%Nb nanocomposite has similar sorption

[☆]To be presented at MH2000.

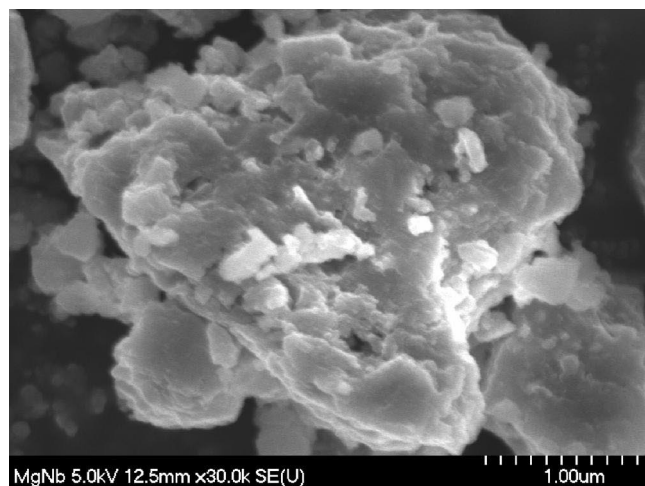
*Corresponding author.

E-mail address: jhuot@ireq.ca (J. Huot).

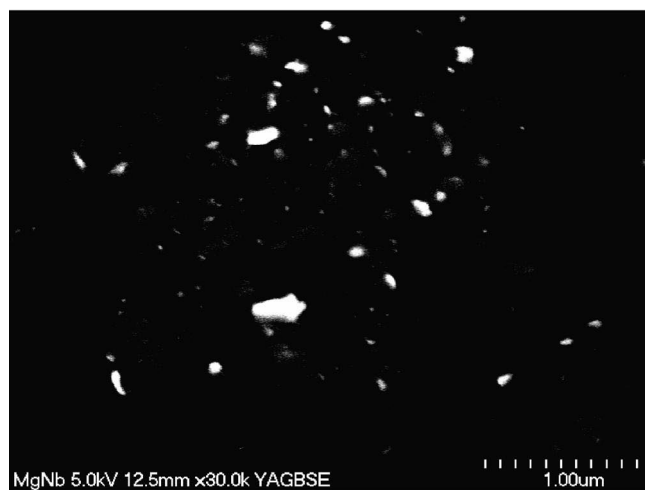
properties as $\text{MgH}_2 + 5\text{at.\%V}$ [10] with non-overlapping X-ray peaks, this system was chosen for further investigation. In this paper, we report the morphology of $\text{MgH}_2 + 5\text{at.\%Nb}$ nanocomposite as shown by SEM and the distribution of niobium particles measured by back-scattered electron images. The phase structure in a desorption/absorption cycle was studied by in-situ X-ray diffraction under hydrogen pressure. Synchrotron radiation was used to observe real-time structural changes during hydrogen desorption.

2. Experimental details

Pure magnesium hydride (95 wt.% MgH_2 , 5 wt.% Mg) from Th. Goldschmidt was mixed with 5 at.% of niobium powder (200 mesh, 99.8%) from Cerac. The mixture was



(a)



(b)

Fig. 1. SEM micrographs of ball-milled $\text{MgH}_2 + 5\text{at.\%Nb}$: (a) secondary electron image; (b) backscattered electron image (the white marks are niobium particles).

milled under argon for 20 h in a hardened steel crucible using a Spex 8000 model shaker mill. The ball to powder weight ratio was 10:1. Field emission scanning electron micrographs were taken on a Hitachi model S4700 and backscattered electrons were detected with a Centaurus apparatus.

X-ray powder diffraction under hydrogen pressure was performed on a Philips X'pert system ($\text{Cu K}\alpha$ radiation) with an Anton Paar XRK9000 pressurized sample holder. Before measurement, the system was pumped and flushed with hydrogen three times before establishing a 1-bar hydrogen pressure. The temperature of the sample holder was then increased from 323 to 623 K in 100-K steps. At each step X-ray powder diffraction was measured. At 623 K, the sample was completely dehydrided. It was rehydrided by reducing the temperature down to 323 K in 100-K steps and taking a diffraction pattern at each step. A beryllium film 0.1-mm thick was put on the sample in order to prevent powder movement during hydrogen desorption/absorption cycle. The X-ray diffraction patterns were analyzed by the Rietveld method using FULLPROF software [11]. Diffraction lines due to beryllium film and magnesium oxide were removed for analysis. Lattice parameters, phase abundance, crystallite size and strain were extracted from the Rietveld refinement output.

Time resolved X-ray diffraction was performed using the synchrotron radiation on the MIT-McGill-IBM beamline at the Advance Photon Source (APS). The beamline flux is 5×10^{12} photons per second (for a nominal storage ring current of 100 mA) and the monochromatic X-rays have an energy of 7.66 keV. A linear photo-diode array detector (PSD) covering an angle of 20° in 2θ collected the scattered X-rays. A pattern could be acquired every 5 ms. Further details of this set-up are given in Ref. [12].

3. Results and discussion

3.1. Morphology and niobium distribution

Fig. 1 shows SEM images of $\text{MgH}_2 + 5\text{at.\%Nb}$ nanocomposite synthesized by ball milling. The powder is porous and is an agglomeration of small particles. The niobium is evenly distributed in magnesium as shown in the backscattered image (Fig. 1b). The histogram of this distribution is presented in Fig. 2 where the particles are grouped according to their average diameter. A normal distribution fitting gives a mean average diameter of 63 nm.

3.2. Structural changes in hydrogen desorption/absorption cycle

Fig. 3 shows the evolution of X-ray diffraction pattern during hydrogen desorption/absorption cycle. The first pattern at 323 K reveals the structure of as ball-milled

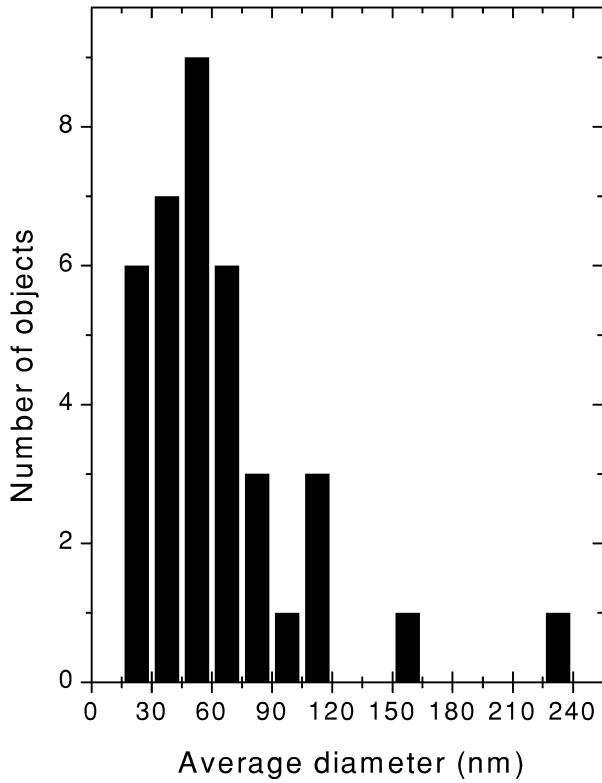


Fig. 2. Niobium distribution in MgH₂ + 5at.%Nb ball milled for 20 h.

powder. It contains tetragonal β-MgH₂ and metastable orthorhombic γ-MgH₂ phases. The metastable γ-MgH₂ phase is formed during ball milling as previously reported when milling magnesium hydride [4,6,8]. The peaks are broad, indicating the nanocrystalline nature of the milled

Table 1

Phase abundance, crystallite size and strain deduced from Rietveld refinement of X-ray diffraction pattern of ball-milled MgH₂ + 5at.%Nb taken at 323 K under 1 bar of hydrogen

Parameter	β-MgH ₂	γ-MgH ₂	β-NbH
Phase abundance (wt.%)	61 (1)	25 (1)	14.0 (3)
Crystallite size (nm)	8.3 (3)	11.2 (9)	30 (3)
Strain (%)	0.7 (7)	1.1 (7)	1.6 (2)

Values in parentheses are 1 S.D.

powder. Table 1 shows phase abundance, crystallite size and strain of each phase as extracted from Rietveld analysis. For niobium hydride, the 14 wt.% phase abundance translates to 4.4 at.%, which is quite close to the nominal abundance of 5 at.% and proves the correctness of the Rietveld analysis. From Table 1, we see that only β-NbH phase has significant strain. However, its crystallite size is bigger than β-MgH₂ and γ-MgH₂ phases.

The diffraction pattern at 423 K is almost identical to 323-K pattern and the crystallographic parameters do not show important changes. At 523 K the γ-MgH₂ phase starts to transform to β-MgH₂. The phase abundance of γ-MgH₂ phase is smaller (22.2±0.8 wt.%), while the β-MgH₂ has a corresponding increase of phase abundance. In polycrystalline materials, the transformation γ→β-MgH₂ occurs at higher temperature (623 K) [13]. At 623 K the sample is almost completely desorbed. Only a small amount (1.6±0.3 wt.%) of β-MgH₂ is still present. The β-NbH phase is still strained (1.3±0.2%). When the temperature is reduced to 523 K, the sample is re-hydrated with a proportion of β-MgH₂ of 69±1 wt.% and of Mg of 14±1 wt.%. With lowering of temperature, β-NbH crystallite size slowly increases to reach 56±5 nm at 323 K.

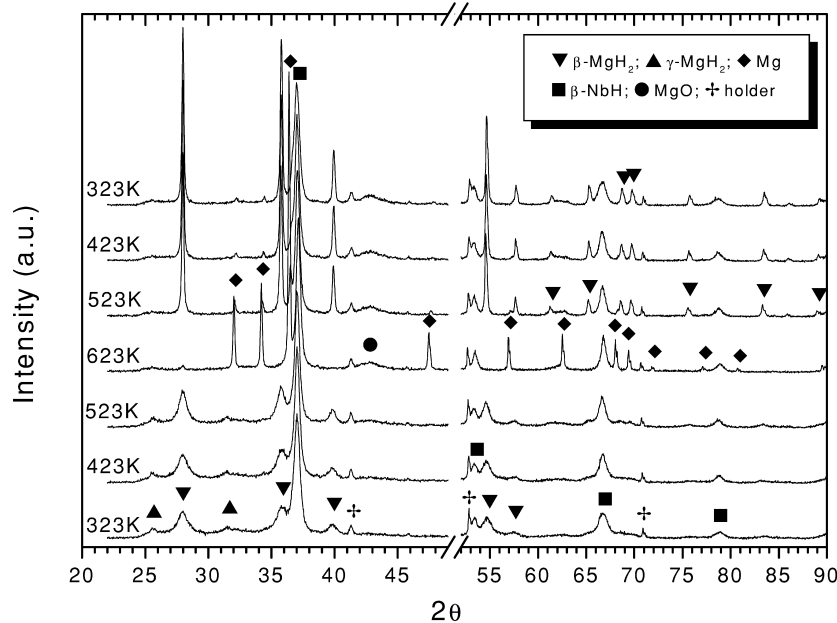


Fig. 3. X-ray powder diffraction pattern under 1 bar of hydrogen of ball-milled MgH₂ + 5at.%Nb during dehydrating/rehydrating cycle. The sequence of X-ray patterns is from bottom to top of the graph. Part patterns where a strong diffraction line is coming from the beryllium film are removed.

This coherent length has to be compared to the mean average diameter of 63 nm of niobium particles found from SEM micrographs. The similarity of these two numbers means that, on average, after one desorption/absorption cycle each niobium particle is totally coherent.

3.3. Real time synchrotron measurement

Fig. 4 shows time-resolved X-ray spectra of $\text{MgH}_2 + 5\text{at.}\% \text{Nb}$ nanocomposite. In this figure, the scattering intensity of the sample through the desorption is represented by a gray-scale contour plot as it is being heated. For clarity, the peaks of the initial and final stages are respectively labeled below and above the image. Desorption started when the temperature reached $\sim 275^\circ\text{C}$ (after 370 s) and was completed within ~ 100 s. When $\beta\text{-MgH}_2$ phase starts to desorb to Mg, a new NbH_x phase becomes visible. This new metastable phase is present for ~ 180 s just before being transformed into metallic niobium. From X-ray peak positions, the hydrogen composition of this

new metastable Nb hydride is estimated to be $\text{NbH}_{0.6}$. This concentration is close to the ϵ phase (Nb_4H_3) which is an ordering of vacancies on a hydrogen sublattice of the β phase [14]. Also, at a concentration of $\text{H}/\text{Nb} \approx 0.6$, the diffusion coefficient of hydrogen reaches a maximum [15]. This new metastable hydride could be viewed as an ordered structure formed by H vacancy ordering. The empty sites in the Nb hydride structure seem to act as channels through which hydrogen flows before being released from the nanocomposite. This is clear evidence that in the desorption process, hydrogen from magnesium hydride flows through the niobium hydride phase. To our knowledge, this is the first direct evidence of the mechanism of hydrogen desorption in such metal hydride. More details about this experiment are reported in Ref. [16].

4. Conclusion

The result of ball milling $\text{MgH}_2 + 5\text{at.}\% \text{Nb}$ mixture is the formation of a nanocomposite with niobium evenly distributed in the magnesium hydride matrix with an Nb average particle diameter of 63 nm. The crystallite sizes of $\beta\text{-MgH}_2$, $\gamma\text{-MgH}_2$, and $\beta\text{-NbH}$ in the as-ball milled powder are, respectively, 8.3, 11.2 and 30 nm. After one dehydrogenation/hydrogenation cycle, the $\beta\text{-NbH}$ crystallite size grows to 56 nm to match the niobium particle size. Based on time-resolved X-ray measurements, we were able to identify the hydrogen desorption mechanism. In this mechanism, a metastable niobium hydride forms during hydrogen desorption with an approximate composition of $\text{NbH}_{0.6}$. Niobium particles act as gateways through which hydrogen flows out of the magnesium hydride.

References

- [1] A. Percheron-Guégan, J.-M. Welter, Preparation of intermetallics and hydrides, in: L. Schlapbach (Ed.), *Hydrogen in Intermetallic Compounds I*, Springer, Berlin, 1988, p. 11.
- [2] A. Zaluska, L. Zaluski, J.O. Ström-Olsen, *J. Alloys Comp.* 288 (1999) 217.
- [3] A. Zaluska, L. Zaluski, J.O. Ström-Olsen, *J. Alloys Comp.* 289 (1999) 197.
- [4] J. Huot, G. Liang, S. Boily, A.V. Neste, R. Schulz, *J. Alloys Comp.* 293–295 (1999) 495.
- [5] A. Zaluska, L. Zaluski, J. Ström-Olsen, R. Schulz, US Patent No. 5,882,623 (March 16, 1999).
- [6] G. Liang, J. Huot, S. Boily, A.V. Neste, R. Schulz, *J. Alloys Comp.* 292 (1999) 247.
- [7] G. Liang, J. Huot, S. Boily, A.V. Neste, R. Schulz, *J. Alloys Comp.* 291 (1999) 295.
- [8] G. Liang, J. Huot, S. Boily, R. Schulz, *J. Alloys Comp.* 305 (2000) 239.
- [9] Z. Dehouche, R. Djaozandry, J. Huot, S. Boily, J. Goyette, T.K. Bose, R. Schulz, *J. Alloys Comp.* 305 (2000) 264.
- [10] R. Schulz, G. Liang, G. Lalande, J. Huot, S. Boily, A.V. Neste, Canada Patent No. PCT/Ca98/00987.

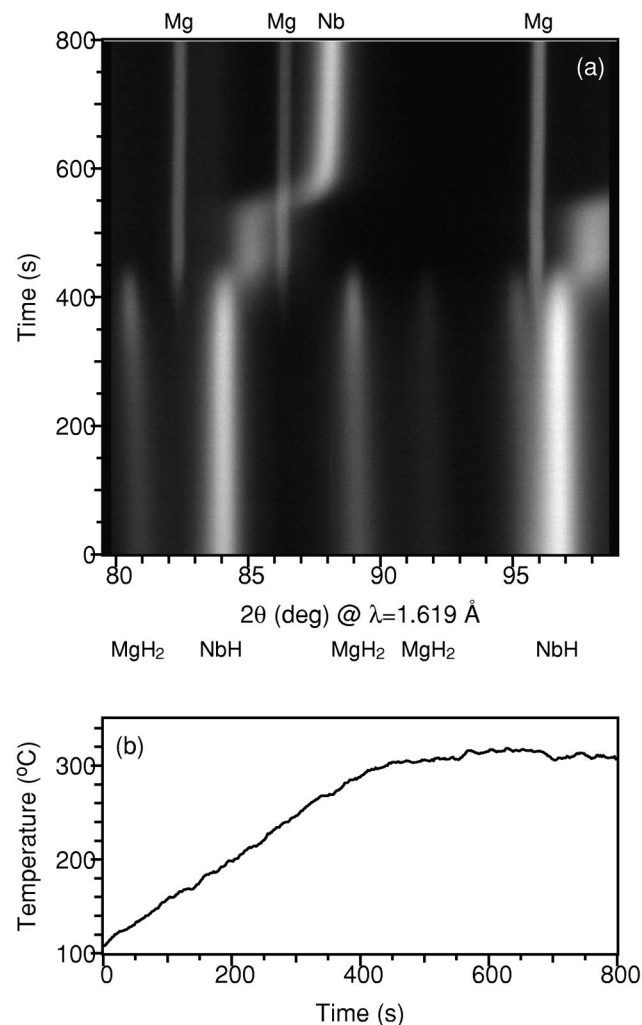


Fig. 4. Time-resolved X-ray scattering data of nanocomposite $\text{MgH}_2 + 5\text{at.}\% \text{Nb}$ during desorption process: (a) raw data; (b) temperature profile.

- [11] J. Rodriguez-Carvajal, Abstracts of the Satellite Meeting on Powder Diffraction of the XV Congress of the IUCr, Toulouse, France, 1990, p. 127.
- [12] J.F. Pelletier, M. Sutton, Z. Altounian, S. Saini, L.B. Lurio, A.R. Sandy, D. Lumma, M.A. Borthwick, P. Falus, S.G.J. Mochrie, G.B. Stephenson, in: P. Pianetta, J. Arthur, S. Brennan (Eds.), AIP Synchrotron Radiation Instrumentation, SRI99, Eleventh US National Conference, 2000, p. 188.
- [13] J.-P. Bastide, B. Bonnetot, J.-M. Letoffe, P. Claudy, *Mater. Res. Bull.* 15 (1980) 1215.
- [14] T. Schober, Vanadium-, niobium- and tantalum-hydrogen, in: F.A. Lewis, A. Aladjem (Eds.), *Hydrogen Metal Systems I, Solid State Phenomena*, Scitec, Zurich, 1996, p. 357.
- [15] Y. Fukai, The metal-hydrogen system, in: U. Gonser (Ed.), *Springer Series in Materials Science*, Vol. 21, Springer, Berlin, 1993, p. 248.
- [16] J.F. Pelletier, J. Huot, M. Sutton, R. Schulz, A.R. Sandy, L.B. Lurio, S.G.J. Mochrie, *Phys. Rev. B* 63 (2000) 521.